JOURNAL OF AGRICULTURAL AND FOOD CHEMISTRY

pubs.acs.org/JAFC Article

X-ray Structure and Molecular Docking Guided Discovery of Novel Chitinase Inhibitors with a Scaffold of Dipyridopyrimidine-3-carboxamide

Pengtao Yuan,[†] Xi Jiang,[†] Siyu Wang, Xusheng Shao, Qing Yang,* and Xuhong Qian*

Cite This: https://dx.doi.org/10.1021/acs.jafc.0c03742 Read Online

ACCESS | Metrics & More | Article Recommendations | Supporting Information

ABSTRACT: Chitinases are the glycosyl hydrolase for catalyzing the degradation of chitin and play an indispensable role in bacterial pathogenesis, fungal cell wall remodeling, and insect molting. Thus, chitinases are attractive targets for therapeutic drugs and pesticides. Here, we present a strategy of developing a novel chemotype of chitinase inhibitors by the construction of planar heterocycles that can stack with conserved aromatic residues. The rational design, guided by crystallographic analysis and docking results, leads to a series of dipyridopyrimidine-3-carboxamide derivatives as chitinase inhibitors. Among them, compound **6t** showed the most potent activity against bacterial chitinase *Sm*ChiB and insect chitinase *Of*Chi-h, with a K_i value of 0.14 and 0.0056 μM, respectively. The strong stacking interaction of compound **6p** with Trp99 and Trp220 found in the *Sm*ChiB−**6p** co-crystal structure verifies the feasibility of our design. Our results provide novel insights into developing potent chitinase inhibitors for pathogen and pest control.

KEYWORDS: *chitinase, inhibitor, X-ray structure, pest control*

INTRODUCTION

Chitin, the second most abundant natural polysaccharide, is the structural component in the coating of many living organisms. It constitutes an indispensable part of the cell wall of fungi, the shells and radulae of mollusc,[1,2] the exoskeletons of arthropods, the sheath of nematodes, protozoan parasites, and the gut lining of many insects. Chitinases are a class of glycosyl hydrolases that catalyze the degradation of chitin. Various biological processes are associated with chitinase inhibition, such as inhibition of cell separation in fungi,[3] toxicity toward insect larvae, and blocking of malaria parasite penetration into the mosquito midgut. Chitinases have thus become attractive targets for pathogen and pest control.[4,5]

Ostrinia furnacalis (Guenée) is the most destructive pest of maize and other pan-pacific areas, causing grain yield losses of ~10% annually.[6] *Of*Chi-h, a molting-indispensable Chi-h from *O. furnacalis*, is a promising target as a result of its exclusive distribution in lepidopteran insects. *Serratia marcescens* is an environmental bacterium that is commonly associated with outbreaks in neonatal intensive care units.[7] *S. marcescens* is also one of the best studied chitinolytic bacteria,[2] making *Sm*ChiB a good molecular-target model for developing chitinase inhibitors. The crystal structures of *Sm*ChiB show that the substrate binds to chitinase through the stacking of the *N*-acetylglucosamine (GlcNAc) units with several conserved aromatic residues. X-ray crystallographic analysis revealed that substrate-competitive inhibitors bind to the substrate-binding site of the enzyme through various interactions, such as $\pi-\pi$ stacking, hydrophobic interactions, and a dense network of direct or water-mediated hydrogen bonds with residues that form the catalytic cavity of the enzyme.

Several natural product chitinase inhibitors have been reported, such as allosamidin, psammaplins, styloguanidines,[8] cyclopentapeptides argifin and argadin,[9] cyclic proline-containing dipeptides, methylxanthine derivatives, and deacetylated chitooligosaccharides.[10] The half maximal inhibitory concentration (IC_{50}) values of those naturally derived inhibitors against numerous chitinases vary from 40 nM to 54 μM. Although some of them are potent inhibitors, their complicated and costly synthesis, limited availability, and unsuitable properties, such as high molecular weight, hampered their widespread use.[11] A few small-molecule inhibitors were found by virtual screening;[12] however, their inhibitory activity was not satisfactory. Therefore, it is of great significance to develop novel chitinase inhibitors with an easily synthesizable scaffold.

Recently, several micromolar polycyclic chitinase inhibitors with planar structures, such as berberine, phlegmacin B_1, FQ1, and TP11,[13−15] have been reported (Figure 1). Molecular docking showed that three of them formed a stacking interaction with aromatic residues in the carbohydrate binding site (berberine with Trp107 of *Of*ChitI, phlegmacin B_1 with Trp160 of *Of*Chi-h, and TP11 with Tyr240 of *Sm*ChiB). With careful analysis of inhibitor−chitinase interactions above, we hypothesized that planar polycyclic compounds with proper

Received: June 14, 2020
Revised: October 20, 2020
Accepted: October 27, 2020

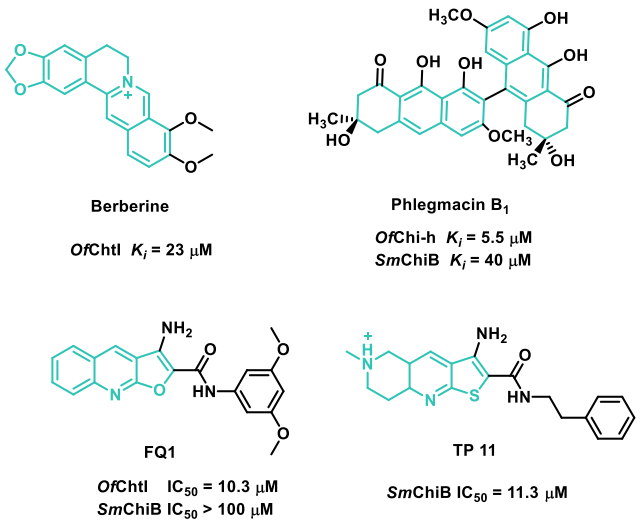

Figure 1. Representative chitinase inhibitors with a planar structure. *Of*ChtI and *Of*Chi-h are chitinases from *O. furnacalis*, and *Sm*ChiB is chitinase from *S. marcenses*.

molecular shape could form hydrophobic stacking interactions with aromatic residues. Therefore, our strategy is to design a series of heterocyclic compounds with ease of synthesis, which may mimic the GlcNAc unit stacking interactions to inhibit chitinase.

Herein, we reported the rational design and synthesis of dipyridopyrimidine-3-carboxamide scaffold chitinase inhibitors, using *Sm*ChiB as a model enzyme of GH18 chitinases (Figure 2). Guided by docking results and the co-crystal complex,

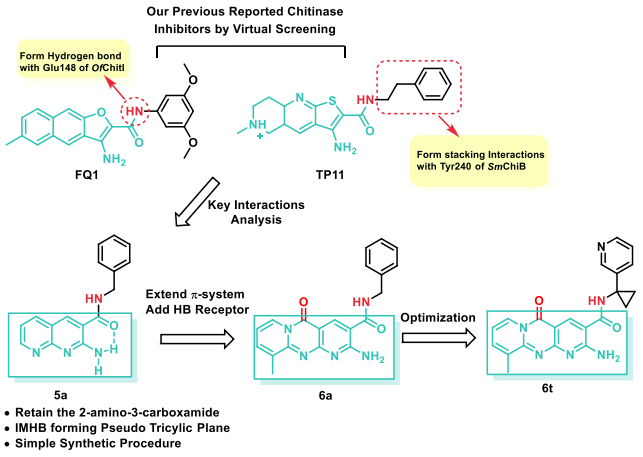

Figure 2. Overview of the rational design and optimization of the novel scaffold of chitinase inhibitors.

compound **6t** was identified as a potent inhibitor of both *Sm*ChiB and *Of*Chi-h. In addition, we revealed the binding mechanism by determination of complex structure *Sm*ChiB–**6p** with 2.0 Å resolution.

MATERIALS AND METHODS

Instruments and Chemicals. Unless otherwise noted, standard and analytical-grade reagents and solvents were obtained from commercial sources and used without further purification. All reactions were carried out under an air atmosphere. Melting points (mp) were recorded on a Büchi B540 apparatus (Büchi Labortechnik, Flawil, Switzerland) and are uncorrected. High-resolution electron mass spectrometry (HRMS) was performed on a Waters Xevo G2 TOF spectrometer (Milford, MA, U.S.A.). ^{1}H, ^{19}F, and ^{13}C nuclear magnetic resonance (NMR) spectra were recorded on a Bruker AM-400 (^{1}H at 400 MHz, ^{13}C at 100 MHz, and ^{19}F at 376 MHz) spectrometer with deuterated dimethyl sulfoxide (DMSO-d_6) or $CDCl_3$ as the solvent and tetramethylsilane (TMS) as the internal standard. Chemical shifts are reported in δ (parts per million). The following abbreviations were used to explain the multiplicities: s, singlet; d, doublet; t, triplet; q, quartet; and m, multiplet. Coupling constants are expressed in hertz.

General Synthetic Procedure of Target Compounds 5a–5c and 6a–6p. The starting material cyanoacetamides **1a–1s** were prepared from methyl cyanoacetate and corresponding amines under neat conditions at room temperature.[16] Compound **1t** was obtained by amide bond formation between cyanoacetic acid and 1-pyridin-3-yl-cyclopropylamine. Compounds **5a–5c** were obtained by the condensation of 2-aminonicotinaldehyde with corresponding cyanoacetamides **1a**, **1k**, and **1l** in the presence of sodium hydroxide via a Friedländer reaction variation[17] (Figure 3). 2-Hydroxy-9-methyl-4*H*-pyrido[1,2-*a*]pyrimidin-4-one (**2**) was prepared by the condensation of 2-amino-3-picoline and diethyl malonate at 110 °C. 2-Chloro-9-methyl-4-oxo-4*H*-pyrido[1,2-*a*]pyrimidine-3-carbaldehyde (**3**), achieved by reaction with $POCl_3$ in dimethylformamide (DMF), was treated with excess aqueous ammonia in ethanol at 70 °C, afforded the key intermediate 2-amino-9-methyl-4-oxo-4*H*-pyrido-[1,2-*a*]pyrimidine-3-carbaldehyde (**4**). Compounds **6a–6t** followed the same synthetic procedure as for compounds **5a–5c** (Figure 3). The detailed synthetic procedure and characteristics of products were described in the Supporting Information.

Purification and Enzymatic Assay. *Sm*ChiB from *S. marcescens* was expressed in *Escherichia coli* BL21(DE3), and *O. furnacalis* chitinase h (*Of*Chi-h) was overexpressed in *Pichia pastoris*. Both chitinases were purified using immobilized metal ion affinity chromatography as previously described.[18] The expressed proteins were quantified using a bicinchoninic acid (BCA) protein assay kit (TaKaRa Biotech, China), and their purities were determined by sodium dodecyl sulfate polyacrylamide gel electrophoresis (SDS–PAGE). Chitinase activities for *Sm*ChiB and *Of*Chi-h were determined using 4-methylumbelliferyl-*N*,*N*′-diacetyl-β-D-chitobioside [MU-β-$(GlcNAc)_2$] (provided by Prof. Jianjun Zhang of China Agricultural University) as a substrate. The reaction mixtures used for inhibitor screening consisted of 100 μL of 1 nM enzyme, 30 μM MU-β-$(GlcNAc)_2$, 10 μM inhibitor, and 1% DMSO in a 20 mM sodium phosphate buffer (pH 6.0). The reaction in the absence of the inhibitor was used as a positive control. After incubation at 30 °C for 20 min, 0.5 M sodium carbonate was added to the reaction mixture and the fluorescence produced by released 4-MU was quantified with a Varioskan Flash microplate reader (Thermo Fisher Scientific) using excitation and emission wavelengths of 360 and 450 nm, respectively. Experiments were performed in triplicate unless specified otherwise. For IC_{50} determination, the inhibitor concentrations were varied in the above reaction and the amount of 4-MU released was quantified as above. IC_{50} values were obtained by curve fitting using Prism software (GraphPad 6.0). For K_i value determination, the inhibitor concentration was varied in the above reaction and different concentrations of substrate (0–150 μM) were used. The amount of released 4-MU was quantified as above, and the K_i value and mode of inhibition were determined using the Dixon plot.

***In Vivo* Bioevaluation.** *O. furnacalis* were reared using an artificial diet with 16 h of light and 8 h of darkness and a relative humidity of 70–90% at 26–28 °C. Larvae of fourth instar were selected for the feeding experiment. Compound **6p** was dissolved in water and diluted with an artificial diet to a final concentration of 600 μg/mL. In the control group, the artificial diet was treated with the same amount of water. Each group contained 30 individual larvae that were continuously fed until all of the larvae pupated. The data were analyzed by Prism software (GraphPad 6.0).

Molecular Docking. The program database file of compounds **5a** and **6g** was prepared using PRODRG.[19] The ligand-free Protein Data Bank (PDB) file of *Sm*ChiB was prepared by PyMOL[20] (DeLano

https://dx.doi.org/10.1021/acs.jafc.0c03742
J. Agric. Food Chem. XXXX, XXX, XXX–XXX

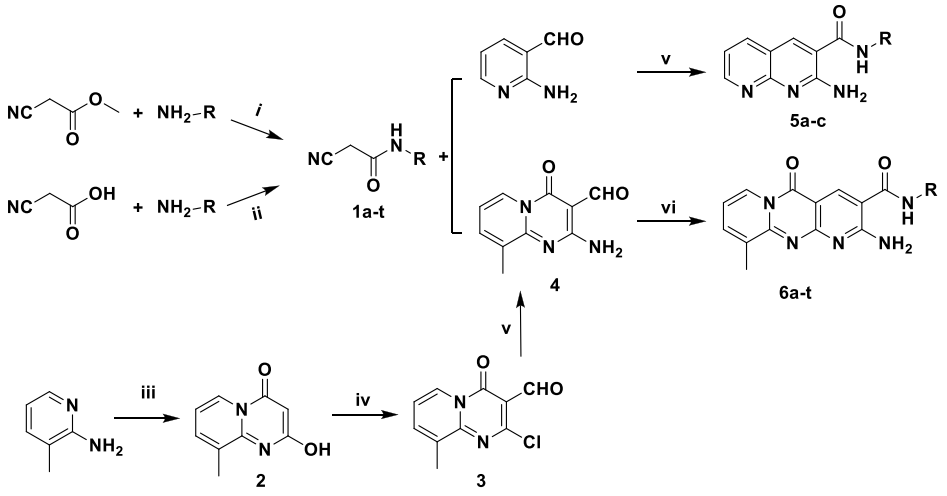

Figure 3. Synthetic route of designed compounds **5a−5c** and **6a−6t**. Reagents and conditions: (i) neat, room temperature; (ii) PyBOP, triethylamine, CH_2Cl_2, room temperature; (iii) neat, 110 °C; (iv) $POCl_3$, DMF, 0−80 °C; (v) aqueous ammonia, EtOH, 70 °C; and (vi) NaOH/EtOH, 70 °C.

Table 1. X-ray Data Collection and Structure Refinement Statistics

	*Sm*ChiB + **6k**	*Sm*ChiB + **6p**
PDB entry	7C92	7CB1
space group	$P2_12_12_1$	$P2_12_12_1$
unit cell parameters		
a (Å)	57.362	55.846
b (Å)	103.644	104.077
c (Å)	186.792	186.286
α (deg)	90	90
β (deg)	90	90
γ (deg)	90	90
wavelength (Å)	0.97776	0.97776
temperature (K)	100	100
resolution (Å)	48.47−2.316 (2.399−2.316)	50.12−1.976 (2.047−1.976)
unique reflections	46796	67805
observed reflections	1267135	123436
R_{merge}	0.04356 (0.09576)	0.04178 (0.09488)
average multiplicity	1.7 (1.3)	1.8 (1.4)
$\langle\sigma(I)\rangle$	9.6 (2)	13.65 (4.92)
completeness (%)	93.56 (62.96)	88 (46)
R/R_{free}	0.1890/0.2268	0.1899/0.2321
protein atoms	7785	7792
water molecules	430	593
other atoms	98	84
rms deviation from ideal		
bond lengths (Å)	0.005	0.014
bond angles (deg)	0.80	1.17
Wilson *B* factor (Å^2)	23.81	23.81
average *B* factor (Å^2)	34.55	27.83
protein atoms	34.21	27.28
water molecules	37.29	33.15
ligand molecules	48.33	41.28
Ramachandran plot (%)		
favored	98.58	98
allowed	1.32	2
outliers	0.10	0

Scientific LLC, San Carlos, CA, U.S.A.) from the inhibitor 26-complexed structure of *Sm*ChiB[21] (PDB code 4Z2G). MGLTools[6] was used to generate the PDBQT files of the proteins and compounds. Affinity grids of 72 × 54 × 76 Å^3 for *Sm*ChiB were calculated using AutoGrid4.[22] Molecular dockings were performed by AutoDock4[22] using the Lamarckian genetic algorithm with a population size of 100 individuals, 25 000 000 energy evaluations, and 27 000 generations. Plausible docking models were selected from

https://dx.doi.org/10.1021/acs.jafc.0c03742
J. Agric. Food Chem. XXXX, XXX, XXX−XXX

the abundant clusters [root-mean-square deviation (RMSD) = 2 Å] that had lower binding energies. Weak intermolecular interactions, such as hydrogen bonding and hydrophobic interactions, were analyzed by LigPlus+[23] and visualized by PyMOL (DeLano Scientific LLC, San Carlos, CA, U.S.A.) and Discovery Studio, client version 20 (Dassault Systèmes, San Diego, CA, U.S.A.).

Crystallization and Data Collection. Protein−inhibitor complex crystals were prepared by co-crystallization methods. For *Sm*ChiB−**6k** and *Sm*ChiB−**6p** crystal complex crystallization, 10 mg/mL protein solution was mixed with an equal volume of well solution containing 5 mM **6k** and **6p**, 5% (v/v) DMSO, 50 mM citrate (pH 5.6), 0.5 M Li_2SO_4, and 0.25 M $(NH_4)_2SO_4$.[24] These crystals were soaked for 10 s in a reservoir solution containing 20% (v/v) glycerol as a cryoprotection reagent and subsequently flash-cooled in liquid nitrogen. X-ray diffraction data of the complexes were collected on BL-19U1 at the Shanghai Synchrotron Radiation Facility in China. The diffraction data of the complexes were processed using the HKL-3000 package.

Structure Determination and Refinement. The structures of *Sm*ChiB−**6k** and *Sm*ChiB−**6p** were solved by molecular replacement with Phaser[25] using the structure of free *Sm*ChiB as a model (PDB entry 4Z2G). The PHENIX suite of programs[26] was used for structure refinement. Coot[27] was used for manually building and extending the molecular models. The stereochemical quality of the models was checked by PROCHECK.[28] The coordinates of *Sm*ChiB−**6k** and *Sm*ChiB−**6p** were deposited in the PDB as entries 7C92 and 7CB1, respectively. The structural figures were generated using the PyMOL program. The statistics for the diffraction data and the structure refinement are summarized in Table 1.

RESULTS AND DISCUSSION

Design and Synthesis of 1,8-Naphthyridine Derivatives 5a−5c. 1,8-naphthyridine derivatives with a planar structure have attracted significant attention for their broad-spectrum biological activities, such as antitumor, antibacterial, anti-inflammatory, and protein kinase inhibition.[29,30] Initially, with key interaction analysis of previously reported chitinase inhibitors FQ1 and TP11, we designed compound **5a** with a simple synthetic procedure as a probe to explore the binding pocket and tested our hypothesis. The 1,8-naphthyridine π system of compound **5a** was expected to form a stacking interaction with aromatic residues in the binding subsites of chitinase. Besides, the amino group could form a pseudo-ring through the intramolecular hydrogen bonding (IMHB) to stabilize the co-plane conformation to fit the binding cleft. Three 1,8-naphthyridine derivatives **5a−5c** were constructed and evaluated their activity against *Sm*ChiB. However, the inhibition activity was not satisfactory. Only compound **5a** showed marginal inhibition against *Sm*ChiB, with 12.6% inhibition activity at 10 μM (Table 2). To further improve inhibition activity, the docking-predicted binding mode of compound **5a** in the *Sm*ChiB active sites was analyzed. A nomenclature for sugar-binding subsites was proposed by Davies et al.,[31] where subsite + n represents a subsite at the reducing end, subsite − n represents a subsite at the non-reducing end, and the cleavage point is between the −1 and +1 subsites. The target region of our molecular docking calculations was based on the position of the substrate in the chitinase crystal structures, which occupies the −1, −2, and −3 subsites of *Sm*ChiB according to the crystal structure, with PDB access code 1E6R. Compound **5a** was predicted to bind in the active site of *Sm*ChiB. However, it seemed that the hydrophobic surface of compound **5a** bicyclic moiety was not big enough to form a strong $\pi-\pi$ stacking to occupy the active site of chitinase (Figure 4). This result prompted us to increase the hydrophobicity of the compounds.

Table 2. Inhibitory Activity of Compounds 5a−5c at 10 μM against *Sm*ChiB

Compd	Structure	Inhibitory activity (%)
5a	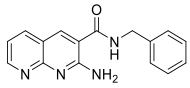	12.6±2.4
5b	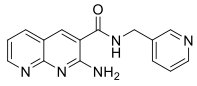	8.8±4.6
5c	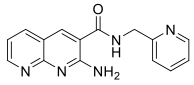	3.8±2.9

Discovery and Modification of Compound 6a. Our strategy was to construct compound **6a** by introducing a rigid pyridine moiety based on compound **5a** to extend the π system and increase hydrophobicity. An additional carbonyl group was expected to form a hydrogen bond with residues in the binding pocket (Figure 2). To realize the simple synthetic procedure, we successfully constructed the key Friedländer synthon **4**, enabling us to obtain compound **6a** by following the same synthetic procedure as the procedure used for the synthesis of compound **5a** (Figure 3).

To our delight, compound **6a** showed good improved activity toward *Sm*ChiB in comparison to compound **5a**. Compound **6a** showed 61.4% inhibitory activity at 10 μM (IC_{50} = 3.7 μM) (Table 3). With the inspiring results, we sought to modify compound **6a** by replacement of the phenyl group with different aromatic heterocycles, substituted phenyl ring, alkyl cycle, alkyl chain, and alkenyl group. First, the methyl group was added in the benzyl position (**6b**), resulting in decreased activity (IC_{50} = 6.3 μM). The additional methyl group may bias compound **6b** toward less bioactive conformation and hamper the hydrophobic interaction with *Sm*ChiB. The substituted phenyl group with F, CF_3, F and Cl, and OMe was also introduced to replace the phenyl group (**6c−6e**). However, none of them improved the activity, indicating that the phenyl ring was not tolerant to substitutions. Then, we replaced the phenyl group with several heterocycles; both **6g** (IC_{50} = 0.77 μM) and **6k** (IC_{50} = 1.18 μM) showed enhanced activity (Table 4). To establish the molecular basis of binding for further design of derivatives, we sought to obtain the co-crystal complex of *Sm*ChiB with compounds **6g** and **6k**. However, only the crystal complex of *Sm*ChiB−**6k** was determined at a resolution of 2.3 Å.

Binding Mechanism of Compound 6k with *Sm*ChiB. Two binding modes were found in the asymmetric unit of *Sm*ChiB−**6k**: two molecules of compound **6k** were bound in the bound +1 and +2 subsites of the binding cleft one protein (Figure S1A of the Supporting Information), and the other protein accommodates only a single compound **6k** (Figure 5A). Although the two-molecule binding mode has been reported[32], our previous isothermal titration calorimetry (ITC) study[33] indicated that only a single inhibitor was bound to chitinase *Sm*ChiB under similar experimental conditions. The existence of the two-molecule binding mode might be due to higher concentrations of compound **6k** used to grow crystals.

https://dx.doi.org/10.1021/acs.jafc.0c03742
J. Agric. Food Chem. XXXX, XXX, XXX−XXX

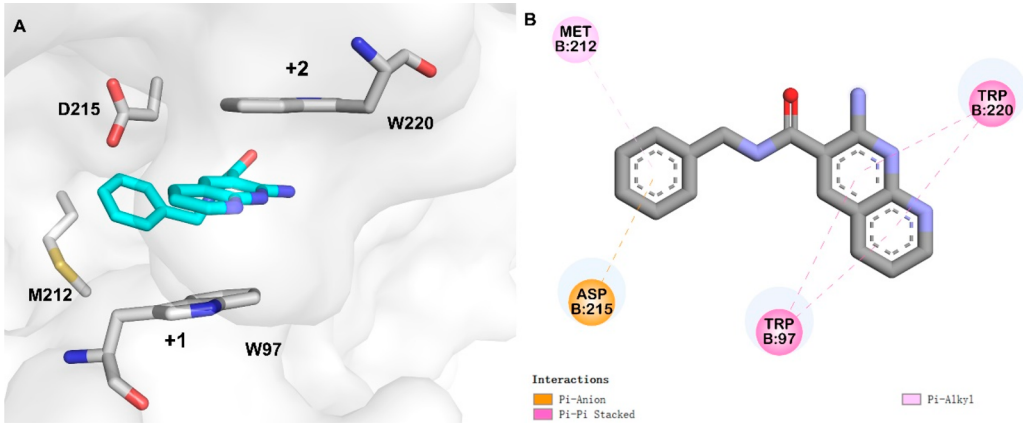

Figure 4. Analysis of the docking result of compound **5a** with *Sm*ChiB: (A) docking-predicated compound **5a** inserted into the +1 and +2 subsites, with compound **5a** shown in cyan, and (B) interactions between compound **5a** and *Sm*ChiB in a two-dimensional (2D) diagram.

Table 3. Inhibitory Activity of Compounds 6a−6j against *Sm*ChiB and *Of*Chi-h

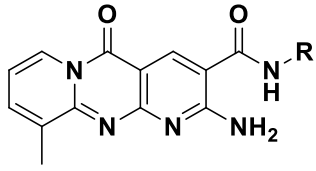

Compd	R	Inhibitory activity at 10 μM (%)[a]	IC_{50} (μM)[a]	Inhibitory activity at 10 μM(%)[b]	IC_{50} (μM)[b]
6a		64.1±3.5	3.70±0.28	84.3±0.4	2.05±0.07
6b		54.9±0.7	6.30±0.40	72.4±2.3	2.62±0.21
6c		30.6±2.8	>10	62.0±1.0	ND
6d		44.3±4.5	>10	14.4±0.5	>10
6e		31.6±12.5	>10	16.4±0.8	>10
6f		16.5±3.9	>10	60.2±4.3	ND
6g		90.9±0.2	0.77±0.20	52.4±5.9	6.17±0.17
6h		56.2±3.0	8.08±1.15	95.6±0.3	0.22±0.04
6i		23.7±2.3	>10	-	>10
6j		16.4±11.0	>10	23.6±1.2	>10

[a]Against *Sm*ChiB. [b]Against *Of*Chi-h. ND = not determined.

Thus, only the single molecule binding mode will be discussed. Two conformations of compound **6k** were found in the binding site (Figure 5A): the pyridopyrimidine moiety of compound **6k** was stacked with tryptophan residues of Trp97 and Trp220, while the 3-pyridine moiety was in the opposite direction. The 3-pyridine moiety of lower conformation was embedded in the hydrophobic region of the binding cleft composed by Tyr10, Phe51, Tyr214, and Trp403. A hydrogen bond was also formed between the 3-pyridyl nitrogen atom with key catalytic residue Glu144, which accounted for the increased inhibitory activity in comparison to compound **6a**. The nitrogen atom of the 2-amino group was found to form a water-mediated hydrogen bond with the side chain of Glu316. Molecular docking of compound **6g** with *Sm*ChiB (Figure S3A of the Supporting Information) suggests a different binding

https://dx.doi.org/10.1021/acs.jafc.0c03742
J. Agric. Food Chem. XXXX, XXX, XXX−XXX

Table 4. Inhibitory Activity of Compounds 6k−6t against *Sm*ChiB and *Of*Chi-h

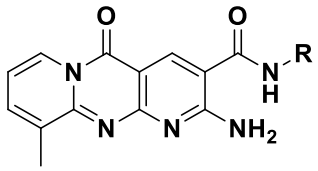

Compd	R	Inhibitory activity at 10 μM (%)[a]	IC_{50}/K_i (μM)[a]	Inhibitory activity at 10 μM(%)[b]	IC_{50}/K_i (μM)[b]
6k		82.7±4.6	1.18±0.06 /1.5	91.8±0.7	0.64±0.08 /0.86
6l		25.8±4.5	>10	55.5±0.8	ND
6m		25.4±3.8	>10	19.1±2.8	>10
6n		64.8±3.1	5.37±0.53	93.9±1.5	0.58±0.04
6o		82.5±1.8	2.90±0.35	78.8±4.2	1.62±0.12
6p		86.2±0.5	0.86±0.08 /0.96	94.4±0.5	0.38±0.02 /0.17
6q		91.9±3.9	0.50±0.12	96.6±0.1	0.30±0.03
6r		72.3±1.8	1.86±0.68	88.7±1.4	0.85±0.06
6s		83.6±3.7	0.87±0.04	91.2±2.1	0.76±0.02
6t		95.0±0.7[c]	0.24±0.01 /0.14	93.4±0.3[c]	0.054±0.002 /0.0056
Allosamidin		ND	-/0.45[d]	ND	ND

[a]Against *Sm*ChiB. [b]Against *Of*Chi-h. [c]At 1 μM. [d]From ref 35. ND = not determined.

mode from compound **6k**, with further validation of the binding mode and modification still undertaken.

Discovery of Compound 6t by Conformation Restriction. With the binding mode of compound **6k**, we sought to modify the pyridinyl group. First, the position of nitrogen in the pyridinyl group was altered, leading to compounds **6l** and **6m** with sharply reduced activity. Replacing 3-pyridinyl with pyrazine **6n** and chlorine-substituted pyridinyl **6o** also led to a decrease of the inhibitory activity. These results suggest that the hydrogen bond between nitrogen in the 3-pyridinyl group with Glu144 of *Sm*ChiB could be important for inhibitory activity.

The existence of the two conformations in *Sm*ChiB−**6k** prompted us to control the conformation by restriction. Preshaping the ligand to the geometry of the binding site could minimize the loss of conformational entropy upon binding and improve the activity accordingly.[34] To lock the 3-pyridine group, an additional methyl group was introduced to create steric hindrance and impose favorable conformation. To our delight, the inhibitory activity of compound **6p** (IC_{50} = 0.86 μM) was improved as expected. To validate the favored configuration of compound **6p**, the *S*-configuration compound **6q** (IC_{50} = 0.5 μM) and *R*-configuration compound **6r** also obtained. Compound **6q** showed 3.7 times the inhibitory activity of compound **6r**, indicating that the *S* configuration is preferred in the inhibition of *Sm*ChiB. To further increase the steric hindrance effect, more sterically demanding groups of ethyl (**6s**) and cyclopropyl (**6t**) were also incorporated. While compound **6s** showed similar inhibition activity as compound **6p**, compound **6t** (IC_{50} = 0.24 μM) showed nearly 4 times the inhibition activity as compound **6p**. The cyclopropyl group augmented the conformational rigidity of compound **6t** and may thus stabilize a favorable binding conformation. The improved activity of compound **6t** may be attributed to the stronger hydrogen bond with Glu144 and the hydrophobic interaction imposed by the cyclopropane ring.

Binding Mechanism of Compound 6p with *Sm*ChiB. To confirm our constriction strategy, the crystal complex of *Sm*ChiB−**6p** was also obtained. The binding mode of complex **6p** is similar to that of complex **6k**, and two binding modes were also found in the asymmetric unit. In the single-molecule binding mode (Figure 5B), only a single conformation existed, which validated our strategy of conformation restriction. Compound **6p** was similarly stacked between Trp97 and

https://dx.doi.org/10.1021/acs.jafc.0c03742
J. Agric. Food Chem. XXXX, XXX, XXX−XXX

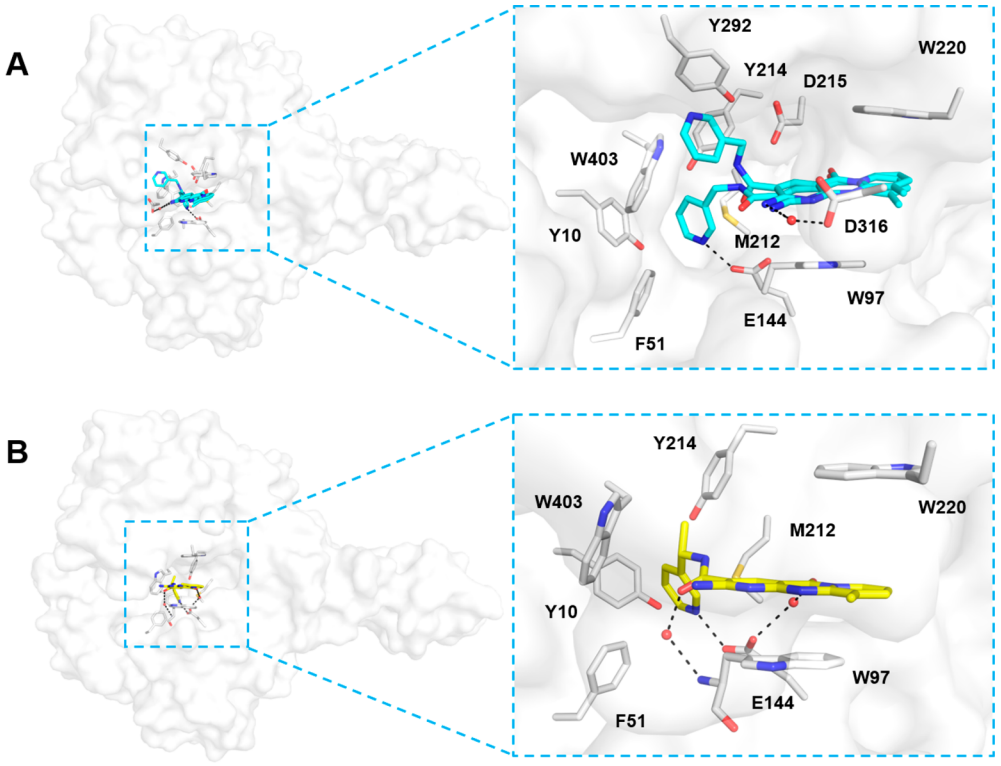

Figure 5. Details of the interaction of compound **6k** with *Sm*ChiB (PDB entry 7C92) and compound **6p** with *Sm*ChiB (PDB entry 7CB1). Compound **6k** is shown in cyan, and compound **6p** is shown in yellow. Hydrogen bonds are shown as black dashed lines, and water molecules are shown as red spheres.

Trp220. Water-meditated hydrogen bonds were observed between the 3-carboxamide oxygen atom with the side chain of Trp97 and the 5-carbonyl group oxygen atom with Glu144, which contributed to the enhancement of inhibitory activity. The key hydrogen bond between the nitrogen atom of the 3-pyridyl group and Glu144 was also observed. In addition, the key hydrogen bond lengths of compounds **6p** and **6k** were 2.59 and 2.63 Å. The stronger hydrogen bond interaction also promoted higher inhibitory activity.

Dixon plots (Figure 6 and Figure S3 of the Supporting Information) showed that compounds **6k**, **6p**, and **6t** are competitive inhibitors of *Sm*ChiB, with K_i values of 1.5, 0.96, and 0.14 μM, respectively. Compound **6t** showed better activity against *Sm*ChiB than allosamidin (K_i = 0.45 μM).[35] The details of both crystal complexes *Sm*ChiB−**6k** and *Sm*ChiB−**6p** support our inhibitor design strategy that the polycyclic scaffold with a proper molecular space can form hydrophobic stacking interactions with aromatic residues in chitinases. Because the key hydrophobic interaction residues Trp99 and Trp220 and key catalytic residue Glu144 are conserved in the most GH18 family chitinases, this strategy could be applied to the discovery of other chitinase inhibitors.

***In Vitro* Inhibition of *Of*Chi-h.** To find the potential application of this scaffold in pest control, the inhibitory activity against lepidoptera-exclusive insect chitinase *Of*Chi-h[36] was also evaluated. *Of*Chi-h has a long and asymmetric substrate binding cleft and shared the conserved residues Trp99, Trp220, and Glu144 with *Sm*ChiB. All of the compounds showed better inhibitory against *Of*Chi-h than *Sm*ChiB, except compound **6g**, supporting our hypothesis of a different binding mechanism of compound **6g** with *Sm*ChiB. Among them, compound **6p** showed good inhibitory activity against *Of*Chi-h, with an IC_{50} value of 0.38 μM. The introduction of more sterically demanding ethyl group compound **6s** (IC_{50} = 0.76 μM) reduced the inhibitory activity. Compound **6t** bearing a cyclopropane ring showed a significant increase, with IC_{50} = 0.054 μM. It was also worth noting that compound **6h** with a furan ring showed good activity against *Of*Chi-h, with IC_{50} = 0.22 μM, suggesting a different optimization direction. These results suggested that dipyridopyrimidine-3-carboxamides could better bind to the *Of*Chi-h.

Molting Inhibiting Effect of Compound 6p on *O. furnacalis*. Compound **6p** was chosen as the representative in the *in vivo* test. When the fourth larvae were exposed to compound **6p**, a decrease in the molting process was observed in comparison to the control group. The average molting time of the treated group was 92 h, while the average molting time of the control group was 81.3 h (Figure 7). The molting inhibiting effect of compound **6p** promises this scaffold as a potential insect growth regulator. Because the water solubility of this scaffold was not satisfying, further optimization toward enhancing their solubility in water may also improve their molting inhibiting effect.

In summary, a series of dipyridopyrimidine-3-carboxamide analogues were rationally designed and optimized. By enhancing the $\pi-\pi$ stacking interaction, we found that compound **6k** showed good inhibitory activity against *Sm*ChiB, with a K_i value of 1.5 μM. Guided by the X-ray structure and restriction of the conformation of compound **6k** by introducing sterically demanding groups led us to obtain compound **6t** with a K_i value of 0.14 μM against *Sm*ChiB. Potent inhibition of Asian corn borer chitinase *Of*Chi-h with a K_i value of 0.0056 μM makes compound **6t** a promising

https://dx.doi.org/10.1021/acs.jafc.0c03742
J. Agric. Food Chem. XXXX, XXX, XXX−XXX

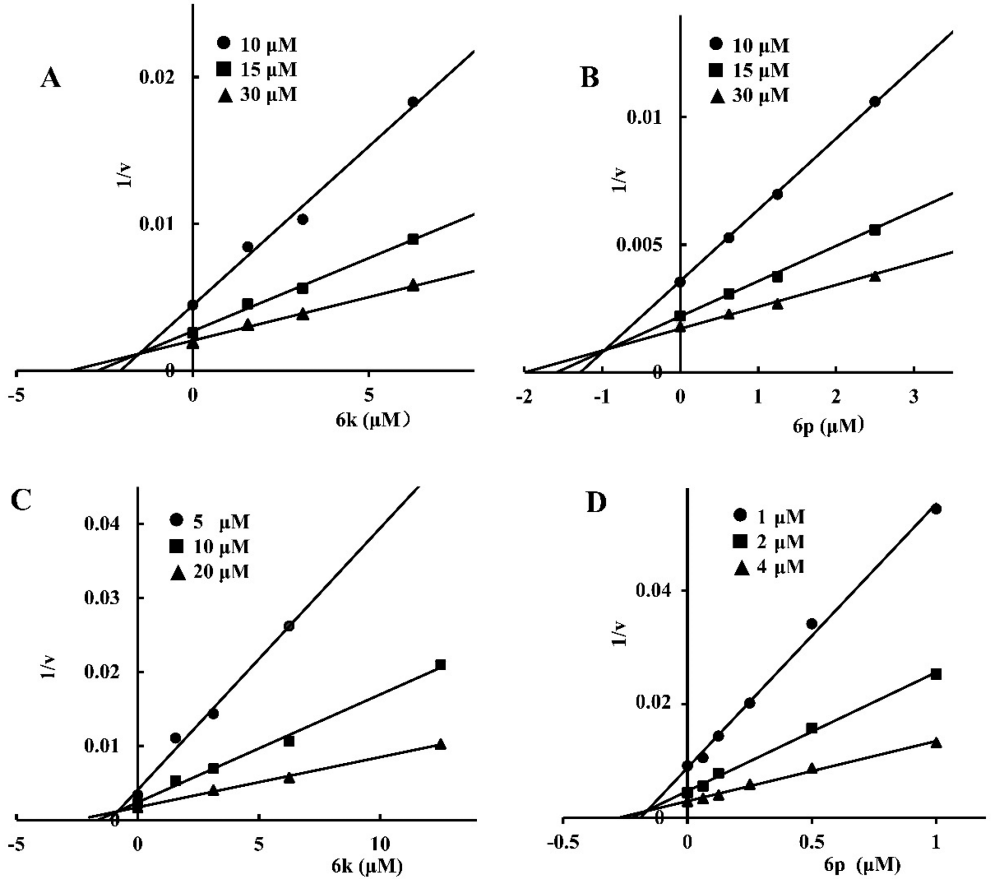

Figure 6. Representative Dixon plots for inhibition chitinase *Sm*ChiB by (A) compound **6k** and (B) compound **6p** and chitinase *Of*Chi-h by (C) compound **6k** and (D) compound **6p**. The trend lines represent three substrate concentrations.

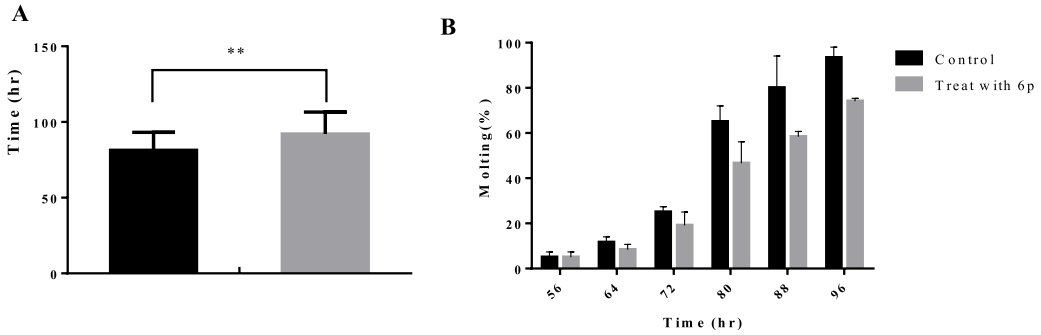

Figure 7. Molting inhibiting effect of compound **6p** on *O. furnacalis*. (A) Average molting time of *O. furnacalis* after exposure to compound **6p**. (**) $p < 0.05$. (B) Time curves of the *O. furnacalis* molting process after exposure to compound **6p**. Each point represents the mean [standard deviation (SD)] of three assays counting the number of molting larvae, and the mean was obtained. Compound **6p** was dissolved in water and diluted with an artificial diet to a final concentration of 600 μg/mL. The larvae were kept in 25 mL plastic cups individually and were continuously fed until all of the larvae pupated.

starting point in future pest management. The complex structure *Sm*ChiB−**6p** revealed that compound **6p** stacked with conserved residues Trp97 and Trp220 and formed a hydrogen bond with Glu144. Thus, this scaffold could be a good template in broad-spectrum chitinase inhibitor design.

■ ASSOCIATED CONTENT

Supporting Information

The Supporting Information is available free of charge at https://pubs.acs.org/doi/10.1021/acs.jafc.0c03742.

Two-molecule binding mode of compounds **6k** and **6p** (Figure S1), docking results of compound **6g** with *Sm*ChiB (Figure S2), Dixon plots for inhibition chitinase *Sm*ChiB and chitinase *Of*Chi-h by compound **6t** (Figure S3), and related NMR and HRMS data of intermediates **2**−**4** and target compounds **5a**−**5c** and **6a**−**6t** (PDF)

■ AUTHOR INFORMATION

Corresponding Authors

Qing Yang − *Guangdong Laboratory for Lingnan Modern Agriculture (Shenzhen Branch), Agricultural Genomics Institute*

https://dx.doi.org/10.1021/acs.jafc.0c03742
J. Agric. Food Chem. XXXX, XXX, XXX−XXX

at Shenzhen, Chinese Academy of Agricultural Sciences, Shenzhen 518120, People's Republic of China; orcid.org/0000-0001-8623-7532; Phone: +86-411-84707245; Email: qingyang@dlut.edu.cn

Xuhong Qian − *Shanghai Key Laboratory of Chemical Biology, School of Pharmacy and State Key Laboratory of Bioreactor Engineering, East China University of Science and Technology, Shanghai 200237, People's Republic of China; School of Chemistry and Molecular Engineering, East China Normal University, Shanghai 200241, People's Republic of China;* orcid.org/0000-0001-6777-0673; Phone: +86-21-64251399; Email: xhqian@ecust.edu.cn; Fax: +86-21-64252603

Authors

Pengtao Yuan − *Shanghai Key Laboratory of Chemical Biology, School of Pharmacy, East China University of Science and Technology, Shanghai 200237, People's Republic of China;* orcid.org/0000-0003-4726-6546

Xi Jiang − *Guangdong Laboratory for Lingnan Modern Agriculture (Shenzhen Branch), Agricultural Genomics Institute at Shenzhen, Chinese Academy of Agricultural Sciences, Shenzhen 518120, People's Republic of China*

Siyu Wang − *Guangdong Laboratory for Lingnan Modern Agriculture (Shenzhen Branch), Agricultural Genomics Institute at Shenzhen, Chinese Academy of Agricultural Sciences, Shenzhen 518120, People's Republic of China*

Xusheng Shao − *Shanghai Key Laboratory of Chemical Biology, School of Pharmacy and State Key Laboratory of Bioreactor Engineering, East China University of Science and Technology, Shanghai 200237, People's Republic of China;* orcid.org/0000-0002-2579-7533

Complete contact information is available at: https://pubs.acs.org/10.1021/acs.jafc.0c03742

Author Contributions

†Pengtao Yuan and Xi Jiang contributed equally to this work.

Funding

This work was financially supported by the Key Project of the Shanghai Science and Technology Committee (18DZ1112703), the National Natural Science Foundation of China (31830076), and the Shenzhen Science and Technology Program (KQTD20180411143628272).

Notes

The authors declare no competing financial interest.

■ ACKNOWLEDGMENTS

The authors thank the staff of BL19U1 beamlines at the National Facility for Protein Science Shanghai (NFPS) and Shanghai Synchrotron Radiation Facility, Shanghai, People's Republic of China, for assistance during data collection.

■ ABBREVIATIONS USED

GlcNAc, *N*-acetyl-D-glucosamine; GH, glycoside hydrolase; IMHB, intramolecular hydrogen bonding; *Sm*ChiB, *Serratia marcenses* chitinase B; *Of*ChtI, *Ostrinia furnacalis* chitinase ChtI; *Of*Chi-h, *Ostrinia furnacalis* chitinase Chi-h

■ REFERENCES

(1) Fuhrman, J. A.; Piessens, W. F. Chitin synthesis and sheath morphogenesis in Brugia malayi microfilariae. *Mol. Biochem. Parasitol.* **1985**, *17* (1), 93−104.

(2) Rathore, A. S.; Gupta, R. D. Chitinases from Bacteria to Human: Properties, Applications, and Future Perspectives. *Enzyme Res.* **2015**, *2015*, 791907.

(3) Cabib, E.; Silverman, S. J.; Shaw, J. A. Chitinase and chitin synthase. 1. Counterbalancing activities in cell-separation of Saccharomyces cerevisiae. *J. Gen. Microbiol.* **1992**, *138* (1), 97−102.

(4) Nagpure, A.; Choudhary, B.; Gupta, R. K. Chitinases: In agriculture and human healthcare. *Crit. Rev. Biotechnol.* **2014**, *34* (3), 215−32.

(5) Cohen, E. Chitin synthesis and degradation as targets for pesticide action. *Arch. Insect Biochem. Physiol.* **1993**, *22* (1−2), 245−261.

(6) Jiang, F.; Zhang, T.; Bai, S.; Wang, Z.; He, K. Evaluation of Bt Corn with Pyramided Genes on Efficacy and Insect Resistance Management for the Asian Corn Borer in China. *PLoS One* **2016**, *11* (12), No. e0168442.

(7) Montagnani, C.; Cocchi, P.; Lega, L.; Campana, S.; Biermann, K. P.; Braggion, C.; Pecile, P.; Chiappini, E.; de Martino, M.; Galli, L. Serratia marcescens outbreak in a neonatal intensive care unit: Crucial role of implementing hand hygiene among external consultants. *BMC Infect. Dis.* **2015**, *15*, 11.

(8) Andersen, O. A.; Dixon, M. J.; Eggleston, I. M.; van Aalten, D. M. Natural product family 18 chitinase inhibitors. *Nat. Prod. Rep.* **2005**, *22* (5), 563−79.

(9) Dixon, M. J.; Andersen, O. A.; van Aalten, D. M. F.; Eggleston, I. M. First Synthesis of Argadin: A Nanomolar Inhibitor of Family-18 Chitinases. *Eur. J. Org. Chem.* **2006**, *2006* (22), 5002−5006.

(10) Rao, F. V.; Andersen, O. A.; Vora, K. A.; DeMartino, J. A.; van Aalten, D. M. F. Methylxanthine Drugs Are Chitinase Inhibitors: Investigation of Inhibition and Binding Modes. *Chem. Biol.* **2005**, *12* (9), 973−980.

(11) Rush, C. L.; Schüttelkopf, A. W.; Hurtado-Guerrero, R.; Blair, D. E.; Ibrahim, A. F. M.; Desvergnes, S.; Eggleston, I. M.; van Aalten, D. M. F. Natural Product−Guided Discovery of a Fungal Chitinase Inhibitor. *Chem. Biol.* **2010**, *17* (12), 1275−1281.

(12) Schuttelkopf, A. W.; Andersen, O. A.; Rao, F. V.; Allwood, M.; Lloyd, C.; Eggleston, I. M.; van Aalten, D. M. Screening-based discovery and structural dissection of a novel family 18 chitinase inhibitor. *J. Biol. Chem.* **2006**, *281* (37), 27278−85.

(13) Chen, L.; Liu, T.; Duan, Y.; Lu, X.; Yang, Q. Microbial Secondary Metabolite, Phlegmacin B_1, as a Novel Inhibitor of Insect Chitinolytic Enzymes. *J. Agric. Food Chem.* **2017**, *65* (19), 3851−3857.

(14) Jiang, X.; Kumar, A.; Liu, T.; Zhang, K. Y. J.; Yang, Q. A Novel Scaffold for Developing Specific or Broad-Spectrum Chitinase Inhibitors. *J. Chem. Inf. Model.* **2016**, *56* (12), 2413−2420.

(15) Duan, Y.; Liu, T.; Zhou, Y.; Dou, T.; Yang, Q. Glycoside hydrolase family 18 and 20 enzymes are novel targets of the traditional medicine berberine. *J. Biol. Chem.* **2018**, *293*, 15429.

(16) Wang, K.; Nguyen, K.; Huang, Y.; Dömling, A. Cyanoacetamide multicomponent reaction (I): Parallel synthesis of cyanoacetamides. *J. Comb. Chem.* **2009**, *11* (5), 920−927.

(17) Wang, K.; Herdtweck, E.; Domling, A. Cyanoacetamides (IV): Versatile one-pot route to 2-quinoline-3-carboxamides. *ACS Comb. Sci.* **2012**, *14* (5), 316−22.

(18) Chen, L.; Zhou, Y.; Qu, M. B.; Zhao, Y.; Yang, Q. Fully Deacetylated Chitooligosaccharides Act as Efficient Glycoside Hydrolase Family 18 Chitinase Inhibitors. *J. Biol. Chem.* **2014**, *289* (25), 17932−17940.

(19) Schüttelkopf, A. W.; van Aalten, D. M. F. *PRODRG*: A tool for high-throughput crystallography of protein−ligand complexes. *Acta Crystallogr., Sect. D: Biol. Crystallogr.* **2004**, *60* (8), 1355−1363.

(20) Schrödinger, LLC. *The PyMOL Molecular Graphics System, Version 1.8*; Schrödinger, LLC: New York, 2015.

(21) Sugawara, A.; Maita, N.; Gouda, H.; Yamamoto, T.; Hirose, T.; Kimura, S.; Saito, Y.; Nakano, H.; Kasai, T.; Nakano, H.; Shiomi, K.; Hirono, S.; Watanabe, T.; Taniguchi, H.; Omura, S.; Sunazuka, T. Creation of Customized Bioactivity within a 14-Membered Macrolide

Scaffold: Design, Synthesis, and Biological Evaluation Using a Family-18 Chitinase. *J. Med. Chem.* **2015**, *58* (12), 4984−4997.
(22) Morris, G. M.; Huey, R.; Lindstrom, W.; Sanner, M. F.; Belew, R. K.; Goodsell, D. S.; Olson, A. J. AutoDock4 and AutoDockTools4: Automated docking with selective receptor flexibility. *J. Comput. Chem.* **2009**, *30* (16), 2785−2791.
(23) Laskowski, R. A.; Swindells, M. B. LigPlot+: Multiple ligand-protein interaction diagrams for drug discovery. *J. Chem. Inf. Model.* **2011**, *51* (10), 2778−86.
(24) van Aalten, D. M.; Synstad, B.; Brurberg, M. B.; Hough, E.; Riise, B. W.; Eijsink, V. G.; Wierenga, R. K. Structure of a two-domain chitotriosidase from Serratia marcescens at 1.9-A resolution. *Proc. Natl. Acad. Sci. U. S. A.* **2000**, *97* (11), 5842−5847.
(25) McCoy, A. J.; Grosse-Kunstleve, R. W.; Adams, P. D.; Winn, M. D.; Storoni, L. C.; Read, R. J. *Phaser* crystallographic software. *J. Appl. Crystallogr.* **2007**, *40* (4), 658−674.
(26) Adams, P. D.; Afonine, P. V.; Bunkóczi, G.; Chen, V. B.; Davis, I. W.; Echols, N.; Headd, J. J.; Hung, L.-W.; Kapral, G. J.; Grosse-Kunstleve, R. W.; McCoy, A. J.; Moriarty, N. W.; Oeffner, R.; Read, R. J.; Richardson, D. C.; Richardson, J. S.; Terwilliger, T. C.; Zwart, P. H. *PHENIX*: A comprehensive Python-based system for macromolecular structure solution. *Acta Crystallogr., Sect. D: Biol. Crystallogr.* **2010**, *66* (2), 213−221.
(27) Emsley, P.; Cowtan, K. Coot: Model-building tools for molecular graphics. *Acta Crystallogr., Sect. D: Biol. Crystallogr.* **2004**, *60* (12−1), 2126−2132.
(28) Laskowski, R. A.; Macarthur, M. W.; Moss, D. S.; Thornton, J. M. *PROCHECK*: A program to check the stereochemical quality of protein structures. *J. Appl. Crystallogr.* **1993**, *26* (2), 283−291.
(29) Madaan, A.; Verma, R.; Kumar, V.; Singh, A. T.; Jain, S. K.; Jaggi, M. 1,8-Naphthyridine Derivatives: A Review of Multiple Biological Activities. *Arch. Arch. Pharm. (Weinheim, Ger.)* **2015**, *348* (12), 837−60.
(30) Wissner, A.; Hamann, P. R.; Nilakantan, R.; Greenberger, L. M.; Ye, F.; Rapuano, T. A.; Loganzo, F. Syntheses and EGFR kinase inhibitory activity of 6-substituted-4-anilino [1,7] and [1,8] naphthyridine-3-carbonitriles. *Bioorg. Med. Chem. Lett.* **2004**, *14* (6), 1411−6.
(31) Davies, G. J.; Wilson, K. S.; Henrissat, B. Nomenclature for sugar-binding subsites in glycosyl hydrolases. *Biochem. J.* **1997**, *321* (2), 557−9.
(32) Pantoom, S.; Vetter, I. R.; Prinz, H.; Suginta, W. Potent family-18 chitinase inhibitors: X-ray structures, affinities, and binding mechanisms. *J. Biol. Chem.* **2011**, *286* (27), 24312−23.
(33) Jiang, X.; Kumar, A.; Motomura, Y.; Liu, T.; Zhou, Y.; Moro, K.; Zhang, K. Y. J.; Yang, Q. A series of compounds bearing a dipyrido-pyrimidine scaffold acting as novel human and insect pest chitinase inhibitors. *J. Med. Chem.* **2020**, *63*, 987.
(34) Zheng, Y.; Tice, C. M.; Singh, S. B. Conformational control in structure-based drug design. *Bioorg. Med. Chem. Lett.* **2017**, *27* (13), 2825−2837.
(35) Houston, D. R.; Shiomi, K.; Arai, N.; Ōmura, S.; Peter, M. G.; Turberg, A.; Synstad, B.; Eijsink, V. G. H.; van Aalten, D. M. F. High-resolution structures of a chitinase complexed with natural product cyclopentapeptide inhibitors: Mimicry of carbohydrate substrate. *Proc. Natl. Acad. Sci. U. S. A.* **2002**, *99* (14), 9127.
(36) Liu, T.; Chen, L.; Zhou, Y.; Jiang, X.; Duan, Y.; Yang, Q. Structure, catalysis, and inhibition of *Of*Chi-h, the lepidoptera-exclusive insect chitinase. *J. Biol. Chem.* **2017**, *292*, 2080.

https://dx.doi.org/10.1021/acs.jafc.0c03742
J. Agric. Food Chem. XXXX, XXX, XXX−XXX